

The rapid prototyping of textured amorphous surfaces for the graphoepitaxial deposition of CdTe films using focused ion beam lithography

S. Neretina · R.A. Hughes · G. Stortz · J.S. Preston · P. Mascher

Received: 11 August 2010 / Accepted: 6 December 2010 / Published online: 13 January 2011
© Springer-Verlag 2011

Abstract Cadmium telluride films deposited on amorphous substrates exhibit a grain structure characterized by [111]-oriented grains, but where the in-plane grain orientation is randomized due to the absence of epitaxy. Here, we explore the viability of promoting an in-plane grain alignment through graphoepitaxy. Fifteen different substrate surface textures were fabricated using focused ion beam lithography. This approach allows for the side-by-side deposition of surface textures where both the areal extent and depth of the surface features are varied in a systematic manner. CdTe films deposited overtop these textures show grain structures with dramatic variations, revealing that particular length scales have the most pronounced effect on the grain structure.

1 Introduction

CdTe has emerged as the dominant low-cost thin-film solar cell absorber material with commercial production exceeding 1 gigawatt per annum [1] at costs of less than

\$1/watt [2]. While great strides have been made in advancing CdTe thin-film solar cell technologies it is somewhat telling that the maximum laboratory efficiencies have stalled near 16.5%, showing little in the way of improvement over the past 15 years [3]. This situation suggests that incremental improvements are becoming increasingly difficult to attain. Thus, the present situation is one where there exists a rapidly improving commercial technology that will soon be subjected to the same constraints imposed on the most advanced CdTe photovoltaic designs. Such a situation is highly undesirable and warrants fundamental studies which explore innovative approaches with the potential to challenge existing best practices.

The quality of the CdTe thin films used in photovoltaic applications is, by any objective measure, poor. Its success as a photovoltaic material stems not from its crystalline perfection, but from the solar cell's insensitivity to the lack of it. The CdTe films have deficiencies on every significant length scale. Low temperature processing gives rise to cracks while high temperatures yield voids and pinholes [4]. In fact, CdTe films used in commercial solar cells are typically five times thicker than their light absorbing properties demand in an effort to minimize this issue [5]. The grain structure itself provides recombination paths, which are deleterious to the cell's performance. The granularity also gives rise to lateral inhomogeneities, which lead to solar cells with spatially varying electrical properties [6]. The microstructure is riddled with stacking faults [7, 8]. Apart from the crystallographic properties, the CdTe films are also difficult to dope, form poor interfaces at both the junction and contact, are difficult to make ohmic contact to [9], and allow for detrimental impurity migration along the grain boundaries [10]. Yet, despite this litany of deficiencies, CdTe films have given rise to the most commercially successful thin-film solar cell technology ever created. Nevertheless, there exists signifi-

S. Neretina (✉) · G. Stortz · J.S. Preston · P. Mascher
Department of Engineering Physics and Centre for Emerging Device Technologies, McMaster University, Hamilton, Ontario, Canada, L8S 4L7
e-mail: neretina@temple.edu
Fax: +1-215-204-4956

R.A. Hughes · J.S. Preston
Brockhouse Institute for Materials Research, McMaster University, Hamilton, Ontario, Canada, L8S 4M1

S. Neretina · R.A. Hughes
Department of Mechanical Engineering, Temple University, 1947 N. 12th Street, Philadelphia, PA 19122, USA

cant evidence that film granularity limits photovoltaic efficiencies [4, 11–13]. Thus, the current situation suggests that much of the potential of this technology remains untapped.

CdTe films for solar cell applications are typically deposited on glass substrates coated with a transparent conducting oxide, which acts as a contact layer. The cell itself consists of a thin-film heterojunction formed between a highly absorbing p-type CdTe layer and a thin transparent n-type CdS film. For the most part, glass is used due to its cost-effectiveness, but its amorphous nature severely impacts film quality due to the absence of an epitaxial relationship. As a result the CdTe films are highly granular, where the exact nature of the granularity depends upon the substrate temperature and processing conditions used [4]. For temperatures below 460°C films have a high propensity for forming grains in the [111] orientation. At higher temperatures a distribution of [111], [220] and [311] grains is observed. For temperatures greater than 520°C, which are typically used in manufacturing processes, random grain orientations are observed. Regardless of the growth temperature used, significant conversion efficiencies are obtained only if the cell is subjected to an empirically discovered process which “activates” the solar cell through the use of a high temperature CdCl₂ treatment [14, 15].

Previously, we reported on the deposition of CdTe films at 300°C using a wide variety of substrate materials [16]. Substrates were chosen such that the degree of epitaxy was varied from nonexistent to excellent. In all instances the film grains grew with their [111]-direction perpendicular to the surface of the substrate due to the preferential growth mode exhibited by CdTe films at this deposition temperature. The in-plane alignment of the grains, however, varied dramatically and was strongly influenced by the degree of epitaxy. C-plane sapphire, which offered the smallest lattice-mismatch to [111]-oriented CdTe, gave rise to a near-perfect grain alignment, while the amorphous surface of glass resulted in in-plane randomness due to the absence of an epitaxial relationship. Other substrates, which offered less favorable epitaxial relationships, gave rise to varying degrees of in-plane alignment, but where the extent of the alignment correlated well with the degree of epitaxy present. From this study it was apparent that a preferential growth mode imposes an out-of plane grain alignment while epitaxy imposes an in-plane alignment. It is noted, however, that exceptions do occur for CdTe where the heteroepitaxial relationship controls both the in-plane and out-of-plane grain alignment [17–20]. Important is the fact that this study also clearly demonstrated deterioration in both the surface morphology of the film and its crystallinity (assessed through x-ray rocking curve analysis) as the degree of in-plane grain alignment is reduced.

From the standpoint of producing CdTe films for solar cell applications, the need for epitaxy is somewhat at odds

with the fact that substrate and contact layer materials are often chosen on the basis of cost and functionality. Increasing the grain alignment in the absence of epitaxy is a fundamental challenge facing not only the solar cell industry but numerous other thin-film technologies. Approaches such as ion beam assisted deposition (IBAD) [21] and oblique angle depositions [22] have positively influenced the grain alignment in other material systems by altering the kinetics of the growth process. An alternate approach is to create an artificial spatially periodic surface relief on the substrate which provides nucleation sites able to promote the growth of a particular grain orientation. In the ideal scenario, these identically oriented grains would grow, merge and unite to form a continuous highly oriented film. Such an approach, commonly referred to as graphoepitaxy [23] or artificial epitaxy [24], has shown much promise with demonstrated successes in semiconductors [25–28], block copolymers [29–31], ferroelectrics [32], metals [33], and biocrystalline films [34]. Here, we present a study where we examine the viability of using the graphoepitaxial approach to alter the grain structure of CdTe thin films.

2 Experimental

2.1 Substrate preparation

Oxidized silicon surfaces were chosen as the substrate for these studies since its flat amorphous surface gives rise to [111]-oriented film grains whose in-plane orientation is completely randomized. While this film-substrate combination is not directly applicable to solar cell applications it does provide an excellent proof-of-principle system for establishing whether graphoepitaxy can significantly alter the grain structure of CdTe films since its flat amorphous surface is unable to promote either real or artificial epitaxy. Thus, changes to the film’s grain structure in the presence of substrate surface texturing can be directly attributed to the influence of artificial epitaxy. It is noted that the use of the graphoepitaxial approach to build upon the partial epitaxy provided by a textured substrate material or a solar cell contact layer could, in fact, give rise to superior CdTe films, but this extra degree of complexity is not warranted for this early stage investigation.

Substrate surface texturing was performed using focused ion beam (FIB) lithography. The technique allows for the micromachining of surfaces with nanometer scale resolution using a focused gallium beam capable of sputtering away selected volumes from the surface. The use of FIB lithography to produce textured surfaces for the purpose of artificial epitaxy is a somewhat novel approach, having only been previously used to alter nanostructure formation [35–38]. From the standpoint of rapidly prototyping numerous surface textures on the same substrate it is superior to

all other commonly used lithographic techniques as it is able to produce textures which modify both the depth and size of side-by-side surface features. This capability allows for the simultaneous film deposition over many surface textures fabricated on a relatively small area, removing possible systematic errors associated with multiple film growths or the uniformity issues which often occur for film depositions over substantial areas. It should be understood, however, that while FIB lithography provides an excellent means for producing small textured areas for proof-of-principle studies, it is impractical for large area surface modifications since it is a time-consuming and expensive procedure. The knowledge gained from such studies, however, will provide direction to efforts aimed at developing low-cost nanoindentation processes [39].

With an amorphous substrate giving rise to [111]-oriented CdTe grains having random in-plane alignment, the intent of any surface texture must be the promotion of in-plane grain alignment. The complete alignment of these grains would give rise to a grain structure, which, when rotated in-plane, would exhibit a threefold symmetry (i.e. the same in-plane symmetry exhibited by a CdTe single crystal). Thus, our initial attempts at developing a surface suitable for the graphoepitaxial deposition of CdTe explored substrate textures comprised of equilateral triangles. If the ledges of these threefold symmetric surface structures were able to nucleate identically oriented grains then the possibility exists for these grains to merge without the need for a grain boundary. Fifteen different surface textures, each comprised of arrays of equilateral triangles and covering an area of approximately $10 \times 10 \mu\text{m}^2$ were fabricated using FIB lithography. Putting many patterns on a single substrate in close proximity ensured that the film growth conditions would be identical for all the textured surfaces. In addition, adjacent areas, which were not altered by the lithography process, provide a flat amorphous surface supporting CdTe film growth which is unaffected by surface texturing. These untextured areas, thus, provide a standard against which films deposited on the textured areas can be judged.

FIB lithography was carried out using a Zeiss 1540XB Focused Ion Beam/Scanning Electron Microscope. The gallium ion beam, controlled with a Nabity NPGS lithography system, had an energy of 30 keV and an ion current of 85 pA. The beam was rastered over each triangular area to within 20 nm of the nominal edge position. Three passes, following serpentine paths, were performed on each triangle, one pass parallel to each face. A final pass along a path 15 nm inside the nominal edge was performed with a line dose of $1.45 \text{ nC}/\text{cm}^2$. All milling was performed in a step and dwell fashion with a 5 nm spacing between points. The surface texture for each of the 15 patterns as well as the unaltered substrate was then characterized using a Digital Instruments Nanoscope III atomic force microscope (AFM) operating in a tapping mode.

2.2 CdTe film deposition

CdTe films were deposited on the textured amorphous surfaces at a deposition temperature of 300°C using the pulsed laser deposition (PLD) technique. The laser used in the process was a GSI-Lumonics Ipex-848 excimer laser operating at 248 nm. The 250 mJ pulses exiting the laser were passed through a mask to obtain the uniform central portion of the beam. The beam was then focused onto a rotating CdTe target to an energy density of $2 \text{ J}/\text{cm}^2$ (laser spot size = $1.5 \times 3 \text{ mm}^2$). The one inch diameter target was grown using the modified Bridgman method [40]. Deposition rates of approximately $1 \mu\text{m}/\text{hour}$ were achieved by operating the laser at a repetition rate of 8 Hz with a substrate to target distance of 3.5 cm. Films were grown to a thickness of 200 nm as determined using a spectroscopic variable angle ellipsometer (Horiba Jobin Yvon, France). All films were deposited in vacuum with a base pressure of 6×10^{-7} Torr.

3 Sample characterization

3.1 Substrate characterization

Figure 1 shows AFM images of the untextured substrate surface (Fig. 1a) as well as the five different texture patterns (Fig. 1b–f) milled into it using FIB lithography. Four of the textures are comprised of an array of equilateral triangles where the values for the triangle side dimension are (b) 300, (c) 400, (d) 500 and (e) 600 nm. The pattern shown in Fig. 1f consists of two superimposed triangular arrays where one triangle has a 500 nm edge dimension and the other has a value of 250 nm. This pattern was generated so as to increase the density of triangular features on the surface. Each pattern was reproduced three times to different milling depths (8, 10 and 12 nm). All of the patterns produced exhibit reasonably sharp edges and corners, but the sputtered areas display, to varying degrees, nanometer scale protrusions.

3.2 Film Characterization

Figure 2 shows AFM images of the CdTe grain structure for films deposited on the substrate surfaces shown in Fig. 1, where the depth of the textured features is 10 nm. Films deposited on textures comprised of triangular arrays with side dimensions of 300 and 400 nm (Fig. 2a–b) show a grain structure which is similar to that obtained for the untextured substrates. For triangular textures having larger side dimensions (Fig. 2d–f) there exists an obvious alteration to the CdTe grain structure where for each of these textures there exists a pattern in the film grain structure that is commensurate with the underlying texture. This pattern is especially

Fig. 1 AFM images of the substrate surface textures fabricated using FIB lithography. The images show the **a** untextured surface and surfaces made up of equilateral triangles with side dimensions of **b** 300 nm, **c** 400 nm, **d** 500 nm, **e** 600 nm and **f** a 250/500 nm mixture. The scale bar is 500 nm

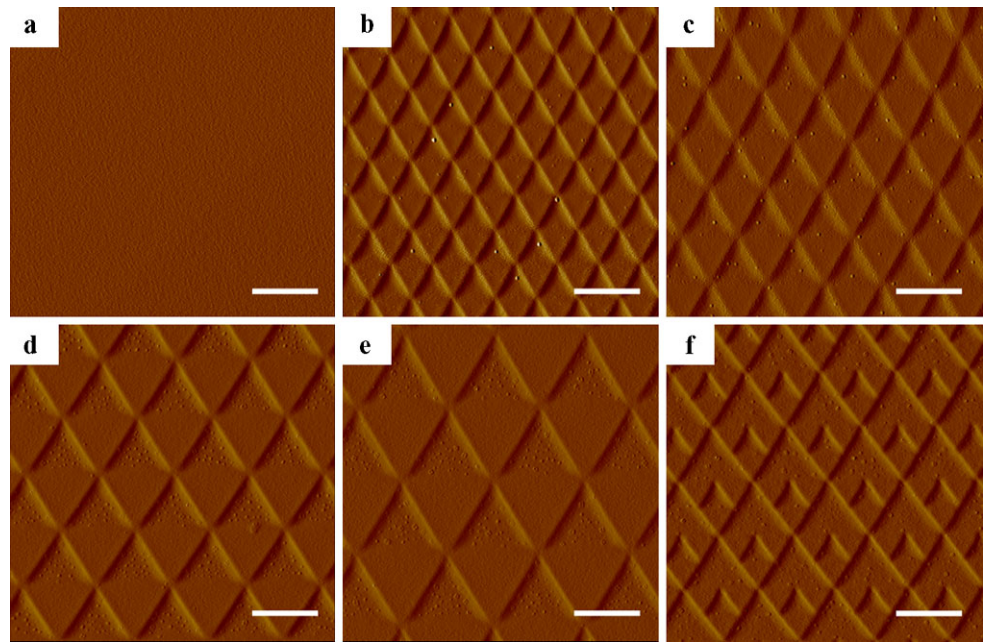
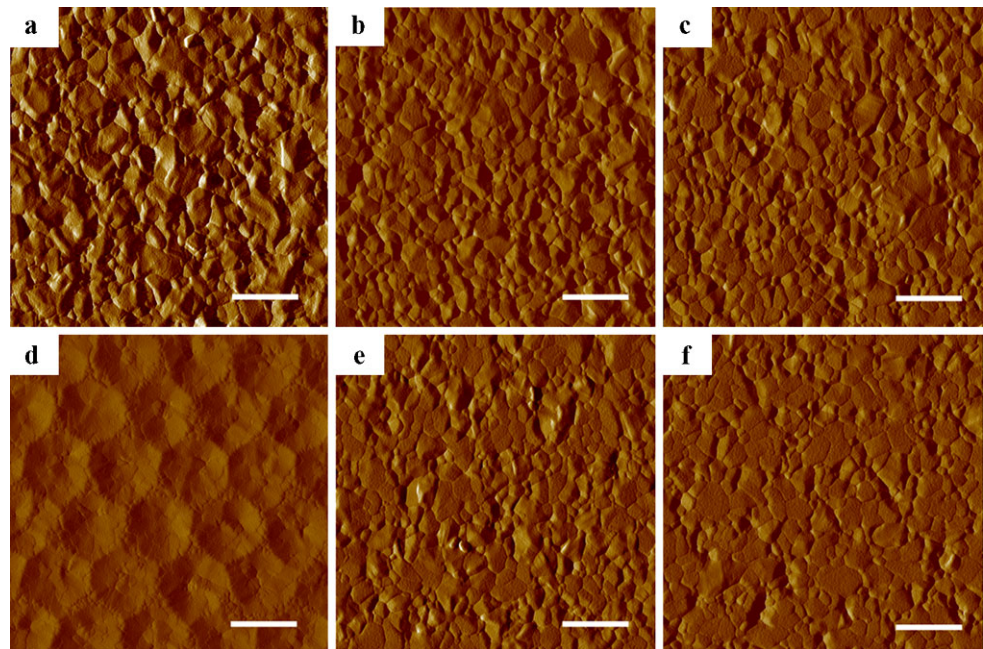


Fig. 2 AFM images of the CdTe film deposited on the textured substrate surfaces shown in Fig. 1. All images are for substrates where the surface texture was milled to a depth of 10 nm. Note that the textures in Fig. 1b–c give rise to a grain structure similar to that derived from the untextured substrate, while the textures in Fig. 1d–f give rise to a significantly altered grain structure. The scale bar is 500 nm



acute for the surface texture comprised of equilateral triangles with a 500 nm side dimension. For this surface texture the film exhibits a grain structure comprised of an array of saucer-like features where there exists one saucer for each triangle milled into the substrate. A similar grain structure is observed when the triangle side dimension is increased to 600 nm, but the pattern is far less discernable. Of considerable interest is a comparison of the film grain structures shown in Fig. 3d, since these substrate surface textures are identical except for the presence of the smaller triangular features. When present, these features result in the complete

elimination of the saucer-like formations, but a grain structure commensurate with the 500 nm triangular array is still clearly visible.

The observed CdTe film grain structure was also strongly influenced by the depth to which the texture was milled into the substrate. Figure 3 shows the CdTe grain structure for films deposited on the 500 nm triangular arrays to depths of 8, 10 and 12 nm. For the smallest depth, the substrate surface texture has little influence on the resulting grain structure of the film. Both the 10 and 12 nm surface textures show the obvious influence of the underlying texture but where,

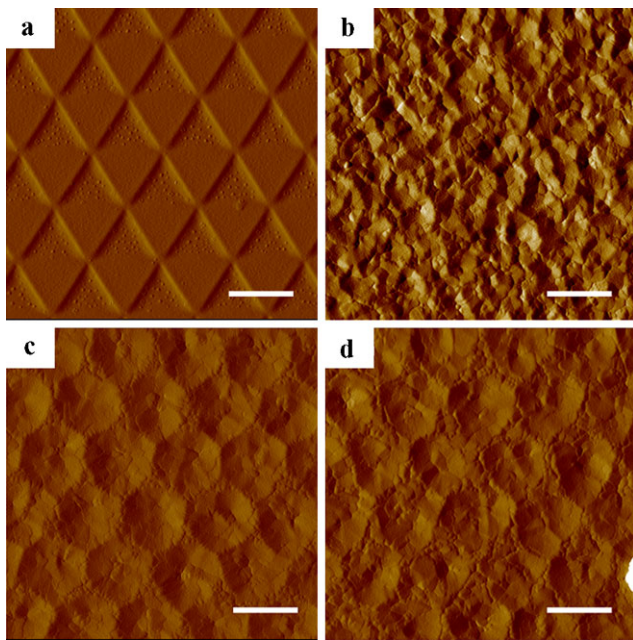


Fig. 3 AFM images showing the influence of substrate surface texture depth on the grain structure of the CdTe film deposited over it. **a** shows the textured surface of the substrate while the remaining images show the CdTe grain structure for films deposited on the substrate surface texture with depths of **b** 8 nm, **c** 10 nm and **d** 12 nm. Note that only the 10 and 12 nm depths give rise to significant alterations to the grain structure of the CdTe film. The scale bar is 500 nm

for the 12 nm case, microcracks appear to form between the ridges of the saucer-like features.

4 Discussion

The results of this study clearly demonstrate that the surface texturing of amorphous substrates can give rise to dramatic alterations in the grain structure of CdTe films. It also reveals that optimum length scales exist where the influence of the texture is most pronounced. For surface textures comprised of arrays of equilateral triangles, the greatest impact on the film grain structure was for milled depths of 10 nm. It should be recognized that such texturing is quite severe, being approximately 40 times greater than the atomic-scale steps formed on miscut (100) silicon which are well-known to strongly influence the in-plane alignment of [111] CdTe grains [41]. In terms of the spatial extent of the texturing, the greatest influence on the grain structure was observed for an array of equilateral triangles with a 500 nm side dimension. While the grain structure produced is commensurate with the underlying substrate surface texture, it seems unlikely that these grain formations arise from a nucleation process which is driven by the edges of the triangle. Such a process would likely lead to threefold symmetric grain formations which are not observed. Instead, it is considered far

more likely that the grains nucleate and emerge from the triangle's corners. In such a scenario, textures based on triangles with small side dimensions offer little advantage since grains would nucleate on length scales similar to or smaller than those observed for the untextured surface. Once the triangle side dimension becomes significantly larger than the grain size, grains will still nucleate at the corners, but the effect will be diminished due to random grain formation elsewhere. Existing between these two extremes would be an optimum triangle side dimension capable of forming a grain structure such as that shown in Fig. 2d.

While these results clearly show that substrate surface texturing impacts the resulting CdTe grain structure, the saucer-like grain formations observed in Fig. 2d are far from ideal. The grain structure is superior to that formed on the untextured surface in that within each saucer-like structure the grains show a strong tendency to merge with each other. Located at the bottom of each saucer-like formation, however, is a round grain approximately 100 nm in diameter. Unfavorable to the films' overall grain structure are the boundaries formed between grains derived from adjacent triangles and which give rise to a network of raised ridges. While such ridges are removed through the addition of the smaller triangles shown in Fig. 1f, they are replaced with undesirable small grains, similar to those formed on the untextured amorphous surface.

Overall, the findings of this first study, which examines the viability of using the graphoepitaxial approach to improve CdTe film quality, are quite encouraging. Much of the potential stems from the strong tendency for CdTe to form [111]-oriented films regardless of the substrate used. This factor, by itself, results in the formation of highly textured films even in the absence of epitaxy. Complementing this natural tendency with an artificial epitaxy, capable of improving the in-plane grain alignment, seems viable based on the results presented here, but where further advancements are needed. The fact that the substrate surface textures used in this work were able to dramatically alter the grain structure, but not in the prescribed manner, suggests that alternate textures are required. With the hypothesis that the corners of the milled triangles are the dominant grain nucleation sites, textures can be generated which take advantage of such features. It should also be recognized that there are numerous measures which have proven effective in altering the heteroepitaxial deposition of CdTe. Such measures, which include (i) the pre-deposition of a tellurium monolayer [41], (ii) selective epitaxy [42–46], (iii) the use of nanostructured materials [47], (iv) polarity control [48, 49], and (v) the use of catalysts [50, 51], all have the potential to be used in concert with the graphoepitaxial approach to further enhance film quality. Increasing the film deposition temperature could also prove beneficial since larger grain sizes will be promoted.

5 Conclusion

CdTe films were deposited on amorphous surfaces which had been textured using FIB lithography. The work clearly demonstrates that the grain structure of the film can be manipulated using methodologies based on artificial epitaxy where both the depth and the areal extent of surface texture features are critical factors in determining the resulting grain structure. Such studies lay the groundwork for the integration of the graphoepitaxial approach into low-cost deposition processes where poor substrate surface quality leads to diminished film properties.

Acknowledgements This work is funded by the Natural Sciences and Engineering Research Council of Canada (NSERC), the Canadian Institute for Advanced Research (CIFAR) and the Ontario Research and Development Challenge Fund (ORDCF) under the auspices of the Ontario Photonics Consortium (OPC). The authors acknowledge the efforts of Dr. Todd Simpson (Western Nanofabrication Facility) and A. Duft (Brockhouse Institute for Materials Research) in the preparation and characterization of the textured surfaces studied.

References

1. First solar becomes first PV company to produce 1 GW in a single year <http://investor.firstsolar.com/phoenix.zhtml?c=201491&p=irol-newsArticle&ID=1365906>, December 15 (2009)
2. First solar passes \$1 per watt industry milestone, <http://investor.firstsolar.com/phoenix.zhtml?c=201491&p=irol-newsArticle&ID=1259614>, February 24 (2009)
3. T. Surek, *J. Cryst. Growth* **275**, 292 (2005)
4. W. Jaegermann, A. Klein, T. Mayer, *Adv. Mater.* **21**, 4196 (2009)
5. E.W. Jones, V. Barrioz, S.J.C. Irvine, D. Lamb, *Thin Solid Films* **517**, 2226 (2009)
6. U. Rau, P.O. Grabitz, J.H. Werner, *Appl. Phys. Lett.* **85**, 6010 (2009)
7. P.D. Brown, J.E. Hails, G.J. Russell, J. Woods, *Appl. Phys. Lett.* **50**, 1144 (1987)
8. A. Romeo, D.L. Batzner, H. Zogg, A.N. Tiwari, *Thin Solid Films* **361–362**, 420 (2000)
9. I.M. Dharmadasa, *Prog. Cryst. Growth Charact.* **36**, 249 (1998)
10. H.C. Chou, A. Rohatgi, N.M. Jokerst, E.W. Thomas, S. Kamra, *J. Electron. Mater.* **25**, 1093 (1996)
11. J.D. Major, Y.Y. Proskuryakov, K. Durose, G. Zoppi, I. Forbes, *Sol. Energy Mater. Sol. Cells* **94**, 1107 (2010)
12. J.R. Sites, J.E. Granata, J.F. Hiltner, *Sol. Energy Mater. Sol. Cells* **55**, 43 (1998)
13. R.W. Birkmire, E. Eser, *Annu. Rev. Mater. Sci.* **27**, 625 (1997)
14. H.R. Moutinho, M.M. Al-Jassim, D.H. Levi, P.C. Dippo, L.L. Kazmerski, *J. Vac. Sci. Technol. A* **16**, 1251 (1998)
15. H.R. Moutinho, R.G. Dhere, M.M. Al-Jassim, D.H. Levi, L.L. Kazmerski, *J. Vac. Sci. Technol. A* **17**, 1793 (1999)
16. S. Neretina, Q. Zhang, R.A. Hughes, J.F. Britten, N.V. Sochinskii, J.S. Preston, P. Mascher, *J. Electron. Mater.* **35**, 1224 (2006)
17. A. Million, N.K. Dhar, J.H. Dinan, *J. Cryst. Growth* **159**, 76 (1996)
18. S. Rujirawat, L.A. Almeida, Y.P. Chen, S. Sivanathan, D.J. Smith, *Appl. Phys. Lett.* **71**, 1810 (1997)
19. S.R. Rao, S.S. Shintri, I.B. Bhat, *J. Electron. Mater.* **38**, 1618 (2009)
20. S. Neretina, R.A. Hughes, G.A. Devenyi, N.V. Sochinskii, J.S. Preston, P. Mascher, *Appl. Surf. Sci.* **255**, 5674 (2009)
21. C.P. Wang, K.B. Do, M.R. Beasley, T.H. Geballe, R.H. Hammond, *Appl. Phys. Lett.* **71**, 2955 (1997)
22. F. Tang, C. Gaire, D.X. Ye, T. Karabacak, T.M. Lu, G.C. Wang, *Phys. Rev. B* **72**, 035430 (2005)
23. E.I. Givargizov, *J. Cryst. Growth* **310**, 1686 (2008)
24. E.I. Givargizov, A.B. Limanov, L.A. Zadorozhnaya, M.A. Lazarenko, I.G. Lukina, *J. Cryst. Growth* **65**, 339 (1983)
25. F. Crnogorac, D.J. Witte, R.F.W. Pease, *J. Vac. Sci. Technol. B* **26**, 2520 (2008)
26. T. Koide, T. Minemoto, H. Takakura, Y. Hamakawa, T. Numai, *J. Appl. Phys.* **97**, 113530 (2005)
27. S.S. Yi, P.D. Moran, X. Zhang, F. Cerrina, J. Carter, H.I. Smith, T.F. Kuech, *Appl. Phys. Lett.* **78**, 1358 (2001)
28. S. Ikeda, K. Saika, Y. Wada, K. Inaba, Y. Ito, H. Kikuchi, K. Terashima, T. Shimada, *J. Appl. Phys.* **103**, 084313 (2008)
29. I. Bita, J.K.W. Yang, Y.S. Jung, C.A. Ross, E.L. Thomas, K.K. Berggren, *Science* **321**, 939 (2008)
30. S.O. Kim, H.H. Solak, M.P. Stoykovich, N.J. Ferrier, J.J. de Pablo, P.F. Nealey, *Nature* **424**, 411 (2003)
31. C. Park, J. Yoon, E.L. Thomas, *Polymer* **44**, 6725 (2003)
32. A.I. Pankrashov, L.A. Zadorozhnaya, E.I. Givargizov, *Sov. Phys. Crystallogr.* **32**, 429 (1987)
33. L.S. Darken, D.H. Lowndes, *Appl. Phys. Lett.* **40**, 954 (1982)
34. E. Givargizov, A.I. Grebenko, L.A. Zadorozhnaya, V.R. Melik-Adamyanyan, *J. Cryst. Growth* **310**, 847 (2008)
35. J. Gierak, *Semicond. Sci. Technol.* **24**, 043001 (2009)
36. S.W. Kim, T. Kotani, M. Ueda, S. Fujita, S. Fujita, *Appl. Phys. Lett.* **83**, 3593 (2003)
37. Y. Morishita, M. Ishiguro, S. Miura, Y. Enmei, *J. Cryst. Growth* **237–239**, 1291 (2002)
38. M. Mehta, D. Reuter, A. Melnikov, A.D. Wieck, A. Remhof, *Appl. Phys. Lett.* **91**, 123108 (2007)
39. E.A. Costner, M.W. Lin, W.L. Jen, C.G. Wilson, C. Grant, *Annu. Rev. Mater. Res.* **39**, 155 (2009)
40. C. Reig, N.V. Sochinskii, V. Muñoz, *J. Cryst. Growth* **197**, 688 (1999)
41. Y. Xin, N.D. Browning, S. Rujirawat, S. Sivanathan, Y.P. Chen, P.D. Nellist, S.J. Pennycook, *J. Appl. Phys.* **84**, 4292 (1998)
42. R. Sporcken, D. Grajewski, Y. Xin, F. Wiame, G. Brill, P. Boieriu, A. Prociuk, S. Rujirawat, N.K. Dhar, S. Sivanathan, *J. Electron. Mater.* **29**, 760 (2000)
43. R. Zhang, I. Bhat, *J. Electron. Mater.* **30**, 1370 (2001)
44. R. Zhang, I. Bhat, *J. Electron. Mater.* **35**, 1293 (2006)
45. T. Seldrum, R. Bommena, L. Samain, J. Dumont, S. Sivanathan, R. Sporcken, *J. Vac. Sci. Technol. B* **26**, 1105 (2008)
46. R. Bommena, C. Fulk, J. Zhao, T.S. Lee, S. Sivanathan, S.R.J. Brueck, S.D. Hersee, *J. Electron. Mater.* **34**, 704 (2005)
47. N. Licausi, W. Yuan, F. Tang, T. Parker, H.F. Li, G.C. Wang, T.M. Lu, I. Bhat, *J. Electron. Mater.* **38**, 1600 (2009)
48. S. Neretina, R.A. Hughes, J.F. Britten, N.V. Sochinskii, J.S. Preston, P. Mascher, *Appl. Phys. A* **96**, 429 (2009)
49. C. Hsu, S. Sivanathan, X. Chu, J.P. Faurie, *Appl. Phys. Lett.* **48**, 908 (1986)
50. S. Neretina, R.A. Hughes, J.F. Britten, N.V. Sochinskii, J.S. Preston, P. Mascher, *Nanotechnology* **18**, 275301 (2007)
51. S. Neretina, R.A. Hughes, G.A. Devenyi, N.V. Sochinskii, J.S. Preston, P. Mascher, *Nanotechnology* **19**, 185601 (2008)